INTERNATIONAL JOURNAL OF MICROWAVE AND OPTICAL TECHNOLOGY,
VOL.20, NO.5, SEPTEMBER 2025

Structural and Optical Characterization of Bis-(4-Hydroxy-1-Naphthyl) Phenylmethanol-Doped Polyvinyl Alcohol Films

Nadhim A. Abdullah[1], Tahseen A. Alaridhee[1] *, Mohammed T. Obeed[1], Haider Abdulelah[1] , Hayder A. Abood[2]

[1]Department of Materials Science, Polymer Research Center, University of Basrah, 61004 Basrah, Iraq

[2]Material Engineering, College of Engineering, University of Basrah, 61004 Basrah, Iraq

E-mail : tahseen.alaridhee@uobasrah.edu.iq

***Abstract*- Consistent Bis-(4-Hydroxy-1-Naphthyl) phenylmethanol (BHP)-doped PVA film was effectively deposited by applying the casting process to prepare several samples with varying concentrations. The BHP: PVA film was analyzed using atomic force microscopy (AFM), which created histograms, distributed intensity assessments, and microscopic surface scanning. The complex aromatic structure of BHP is expected to enhance light absorption and improve electrical conductivity in the PVA matrix. The optical properties were investigated, including absorbance spectrum, optical bandgap, Urbach energy, extinction coefficient, and dielectric function. Doping PVA with BHP reduced the energy gap and increased the Urbach tail as the dye concentration increased, with a reversal of this behavior observed at a 100% BHP concentration ratio. The irregular behavior observed in this study suggests that molecular aggregation becomes effective at high doping degrees, which opens a new way to modify the optical properties of polymer-based films.**

***Index Terms*- Spectroscopy, Optical properties, BHP compound, PVA.**

I. INTRODUCTION

The growing demand for efficient and adaptable optoelectronic devices has sparked advancements in materials research. Synthetic organic dyes have emerged as viable possibilities among these materials due to their remarkable capacity to absorb and emit light, together with their chemical diversity. The properties of synthetic dyes enable use in several applications, including pH indicators, dye-sensitized solar cells, and—most significantly for our focus—optoelectronic devices [1-6]. Recent research has emphasized the exceptional non-linear optical (NLO) features of synthetic dyes, essential for applications in optical switching, light modulation, and signal processing [7-11]. Synthetic compounds, in contrast to conventional inorganic materials, have exceptional plasticity and tunability, facilitating the creation of customized solutions adapted to specific requirements in applications [12-15].

The chemical compound bis-(4-hydroxy-1-naphthyl) phenyl-methanol, an organic compound known as phenolphthalein, has garnered significant interest due to its unique molecular structure and optical properties. Phenolphthalein, commonly utilized as a pH indicator in analytical chemistry, possesses notable absorption and emission properties that make it suitable for many optoelectronic applications. The conjugated structure of phenolic hydroxyl groups could be useful for optical sensors or fluorescent probes because they can act as auxochromes that improve color characteristics, fluorescent probes [16-18], development of new lasers [19, 20],

photodynamic therapy [21-23], and environmental sensing [24, 25]. The synthetic characteristics of phenolphthalein offer modifications that can improve its optical performance, thereby expanding its adaptability in the development of next-generation optoelectronic systems [26-30]. Polyvinyl alcohol (PVA) is an extensively investigated polymer that has several beneficial qualities, such as high dielectric strength, optical transparency, and biocompatibility. These qualities make it useful for a broad range of applications, from biomedical purposes to optoelectronics [31-33]. Doping PVA is a typical way to change its qualities so that it can accomplish certain tasks better.

This study examines the optical characteristics of polyvinyl alcohol (PVA) loaded with phenolphthalein to evaluate its suitability as a material for diverse optoelectronic applications. PVA, a hydrosoluble synthetic polymer, is frequently used as a substrate due to its superior film-forming properties and ophthalmic purity. For the first time, Bis-(4-Hydroxy-1-Naphthyl) Phenylmethanol (BHP) was doped into a polyvinyl alcohol (PVA) matrix to make adaptable thin films using the casting process. This research seeks to enhance the comprehension of synthetic organic compounds in optoelectronics and promote the advancement of efficient, dependable, and cost-effective optical technologies by analyzing the linear optical properties of this composite material using UV-Vis spectroscopy.

II. MATERIALS AND EQUIPMENT

A. Materials

There are two categories of materials used in this investigation (see Fig. 1): We selected the bis(4-hydroxy-1-naphthyl) phenylmethanol from Sigma-Aldrich. Its chemical formula is $C_{27}H_{20}O_3$, and its molecular weight is 392.4459 g/mol. The poly (vinyl alcohol) (PVA) powder material (average molecular weight = 70,000–100,000) was purchased from Himedia Lab. Pvt. Ltd. The preparation process utilized a magnetic stirring device (BOECO Hot Plate Magnetic Stirrer, model MSH 420). The maximum stirring volume of the magnetic stirrer is 15 L, featuring a stirring speed range of 60–1110 rpm and a heating capability of up to 450 °C. We collected the ultraviolet-visible spectra using the GBC Cintra 2020 UV-Visible spectrometer, Australia, which operates in the 200–1100 nm wavelength range.

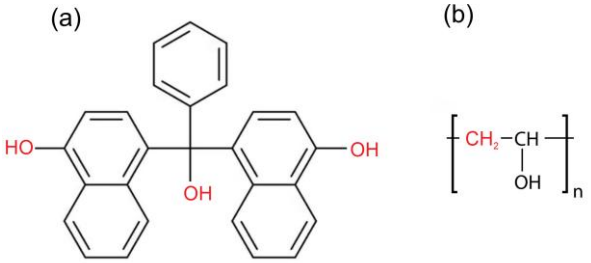

Fig. 1. (a) Structure of (a) $C_{27}H_{20}O_3$ dye and (b) PVA $[-CH_2-CH(OH)-]_n$.

B. Preparation Process of Samples.

Polyvinyl alcohol of 0.5 g dissolved in 10 ml of distilled water and stirred at 80 °C for 120 minutes. Independently, bis-(4-hydroxy-1-naphthyl) phenyl-methanol (0.001 g) was dissolved in 10 ml of ethanol and stirred at 40 °C for 15 minutes. Both solutions were filtered through 0.45-micrometer syringe filters. The dye solution was then progressively mixed into the PVA solution under continuous stirring for 25 minutes to ensure homogeneous adsorption.

Glass substrates were ultrasonically cleaned (35 W) in isopropanol for 5 minutes, rinsed successively with acetone and distilled water, and dried in an oven at 70 °C for 3 hours. The dye-doped PVA solution was cast onto already

Table 1: Composition and thickness of PVA-doped BHP samples.

Sample	PVA Volume (ml)	Dye Volume (ml)	Thickness (μm)
S_o	12.5	0	24
S_1	12.4	0.1	29
S_2	12.1	0.4	36
S_3	11.9	0.6	31
S_4	11.5	1	45

prepared substrates according to the proportions specified in Table 1. The cast films were annealed at 50 °C for 2 hours to induce polymer chain expansion and eliminate residual solvent. Final film thickness, measured using a digital micrometer, was consistent across all samples (Table 1).

III. MORPHOLOGY STUDY

To further show the morphological and structural features of the doped samples, the choice of the AFM device is effective in the polymer field through understanding how filler agglomerates behave in polymer composites. The AFM images (2D and 3D) offer helpful details about the surface morphology of the PVA-doped bis-(4-Hydroxy-1-Naphthyl) phenylmethanol film. As shown in Fig. 2(a), the 2D image exhibits a granular surface texture with a relatively low average roughness, and the contrast variations in the image indicate a nanoscale roughness. Three-dimensional surface topography in Fig. 2(b) shows a viewpoint on the vertical distribution of surface characteristics. The image suggests a somewhat homogeneous distribution of the dopant inside the PVA matrix by lacking signs of major phase separation or large-scale agglomerates. The BHP dye molecules are represented by the microscopic dark regions, while the PVA chains are represented by the shining microscopic regions.

The low roughness of the material makes it an interesting candidate for photonic and optoelectronic systems, where surface homogeneity is crucial for device efficiency. The histogram analysis evaluates the roughness of the BHP: PVA film (see Fig. 2(c)). The statistical distribution of the surface presents a symmetric, nearly Gaussian distribution, indicating a uniform surface profile with

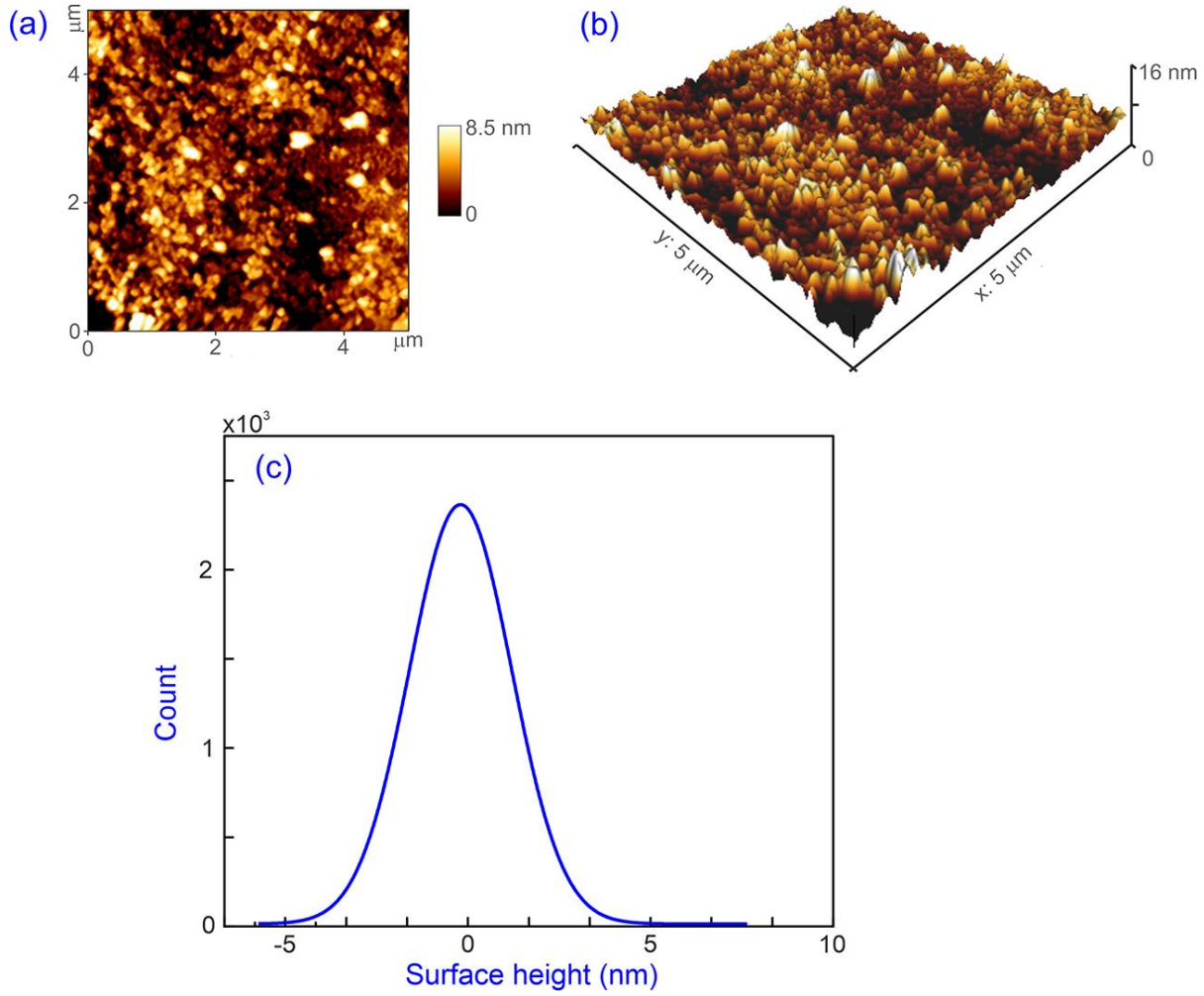

Fig. 2. (a) 2D and (b) 3D AFM images of BHP: PVA with (1 ml of volume) (c) Height distribution of AFM-measured surface topography of the BHP: PVA film.

minimal skewness. Statistical analysis suggests that the film possesses a surface without significant defects or outliers, while the narrow spread of the height distribution confirms the homogeneity, as indicated by the total height variation (R_t) value of 11.5 nm. Furthermore, the AFM-based histogram indicates that the arithmetic mean roughness (R_a) is equal to 1.509 nm, which is a relatively smooth film. On the other hand, the root mean square roughness (R_q=1.932 nm) value indicates the existence of minor surface irregularities. The minimal difference between Ra and R_q suggests a uniform distribution of surface features, rather than the presence of irregular deep valleys.

IV. BASIC THEORY AND ANALYSIS

A. Optical Absorption

By analyzing the optical absorbance spectra, after correcting for reflection, the linear absorption coefficients, α, for PVA film and doped film at different dye concentrations were determined using the Beer–Lambert relation [34-37]:

$$I = I_o\, exp^{(\alpha t)}$$

Therefore,

$$\alpha = \frac{2.303}{t}\log\left(\frac{I}{I_o}\right)$$

$$\alpha = 2.303\left(\frac{A}{t}\right) \quad (1)$$

where *A* represents the absorbance, and *t* is the thickness of the sample. The sample absorbs an extensive amount of light because the photons arriving at the sample have enough energy to transfer electrons from the valence band to the conduction band. This straightforward approach effectively pinpointed the optical absorption edge, shedding insight into the band structure characteristics of the film.

B. Tauc Plot and Optical Band Gap

A crucial physical component of semiconductors and dielectric characteristics is the HOMO-LUMO energy denoted as E_g. To investigate the optical absorption edge, we employed the following relationship, commonly known as Tauc's Technique [38]:

$$\alpha = \frac{T_p\{(h\upsilon - E_g)\}^{\gamma}}{h\upsilon} \quad (2)$$

where T_p is the material-dependent constant, and γ represents the distribution of the density of states reference that typically depends on the nature of the electronic transition (direct (1/2, 2, 3/2) or indirect (1/3)). By rewriting Eq. 2, it can obtain the band gap E_g as:

$$\frac{d[\ln(\alpha h\nu)]}{d(h\nu)} = \frac{m}{h\nu - E_g} \quad (3)$$

Calculating the value of m leads to identifying the type of transition occurring. A break or discontinuity can be obtained at the location derived from Eq. (3) when plotting d[ln(αhν)]/d(hν) against hν. The energy at which discontinuity occurs is the determinant of the band gap, for example. The slope of the curves showing the relationship between ln(αhν) and ln(hν-E_g) assisted in identifying that the value was close to 2 after using the E_g value to calculate *m*.

C. Urbach Energy (Tail States)

The Urbach edge is an indication of disorder in optical materials. It presents a strong, non-destructive method to measure the quality of materials, the number of defects, and how doping or processing conditions affect the optoelectronic behavior of films and composites. The expression of the exponential tail of the absorption edge is defined as [39]:

$$\alpha(h\nu) = \alpha_o \exp\left(\frac{h\nu}{E_u}\right) \quad (4)$$

The symbol α_o stands for the pre-exponential component in the Urbach exponential absorption edge equation. This equation shows how the absorption coefficient α interacts at the absorption edge in materials that are disordered or amorphous.

D. Refractive Index and Extinction Coefficient

Refractive index is one of the key characteristics used to identify the optical properties of a sample. The relationship of Kramers and Kronig has been used to determine the parameter n of pure PVA and the doped sample with different concentrations [40, 41]:

$$n = \frac{1+R}{1-R} + \sqrt{\frac{4R}{(1-R)^2} - k^2} \quad (5)$$

where R and k represent the reflectance spectra and the extinction coefficient, respectively. The extinction coefficient (k) is an important optical property that indicates how much light is absorbed or dispersed as it travels through a material. The extinction coefficient (k) is defined as [42]:

$$k = \frac{\alpha\lambda}{4\pi} \quad (6)$$

D. Dielectric Function

A related characteristic of a substance is the complex dielectric constant, represented as $\varepsilon = \varepsilon_r + \varepsilon_i$, which provides more understanding of its optical properties. The real ε_r and imaginary ε_i components of the dielectric constant are determined using the following equations [43, 44]:

$$\varepsilon_r = n^2 - k^2 \quad (7)$$
$$\varepsilon_i = 2nk \quad (8)$$

V. RESULTS AND DISCUSSION

A. UV-Vis Spectroscopy of PVA-BHP Films

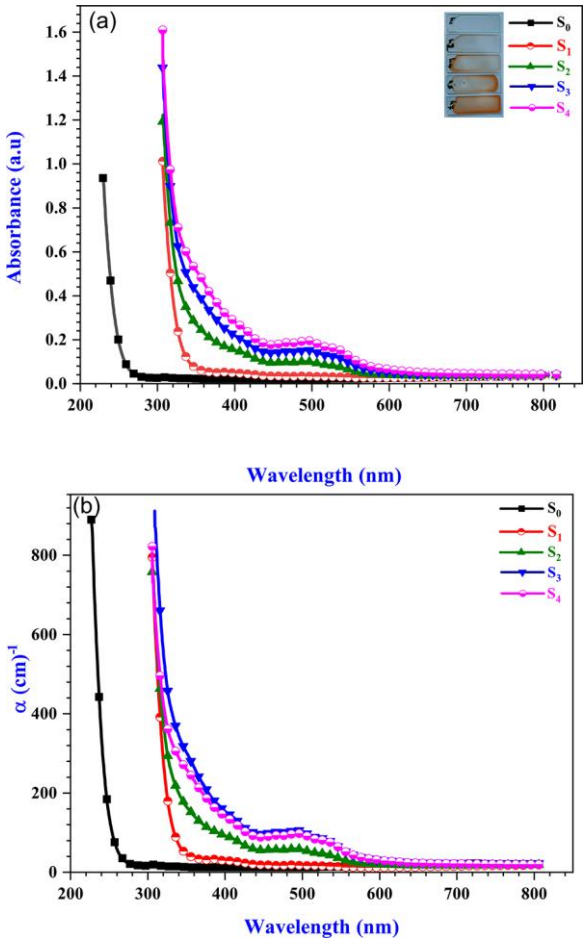

Fig.3. (a) UV-Vis spectra and (b) the absorption coefficient of PVA and BHP-doped samples at various concentrations.

Figure 3(a) depicts the absorbance spectra profile of samples (pure PVA film and doped films with different dye concentrations) exposed to a UV-visible spectrophotometer (CE-7200) with a double beam throughout a wavelength range of 300–900 nm at room temperature. A significant decline is evident in the absorption spectra between 300 and 450 nm for pure PVA, correlating with the band gap of PVA, which shifts to longer wavelengths in the doped samples. The modification of the PVA energy band gap is indicated by the noticeable displacement of the absorption edge for the doped samples. The substance film exhibits its highest absorption value at 489.1 nm, as shown in Fig. 3(a). Even after varying quantities of dye

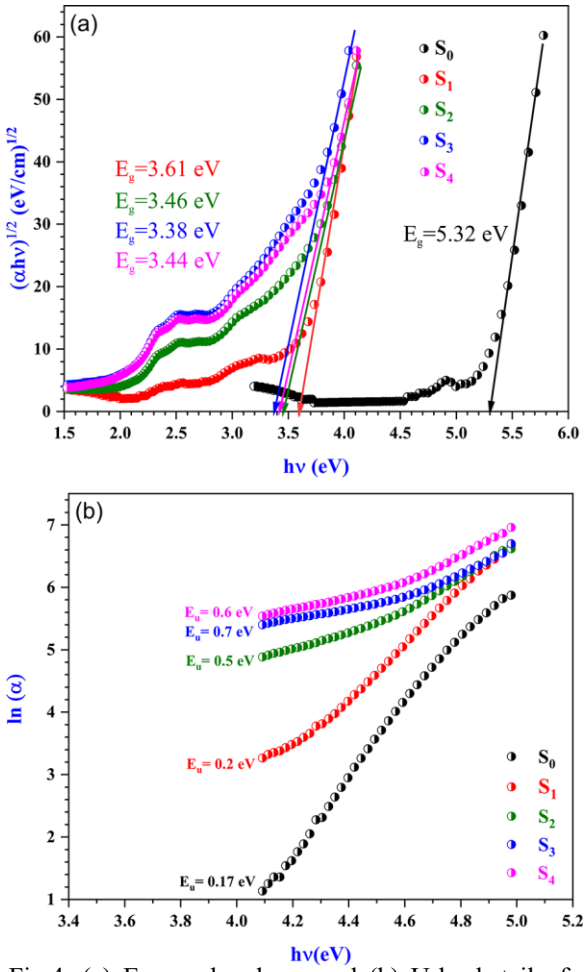

Fig.4. (a) Energy bandgap, and (b) Urbach tail of BHP: PVA samples.

concentration, the spectra of the material film almost always have a constant peak location.

BHP functions as a chromophore, absorbing light in the UV-visible region. Increased BHP concentrations are associated with a higher density of chromophores in the PVA matrix. The increased presence of chromophores intensifies light absorption, resulting in an enhancement of the absorption spectrum. The main absorption peak in Fig. 3(a) can be seen at 489.1 nm, which is caused by the naphthyl groups and hydroxyl groups forming a conjugated π electron system [45]. As can be shown in Fig. 3(b), when the concentration of BHP increases, the absorption edge shifts toward longer wavelengths. The π-π stacking of aromatic groups explains this phenomenon. Dopant molecules become closer to one another in the PVA matrix as the concentration increases, which improves the π-orbital overlap between aromatic rings [46–48]. This reduces the energy gap and causes redshift by delocalizing electronic states.

B. Bandgap and Urbach Energy

The calculation of m-value in Eq. (3) suggests that the fundamental absorption edge is generated by the allowed indirect transitions. It is critical to keep the overall energy and momentum of the coherent electron-photon throughout the transition. Figure 4 shows the behavior of the electrical band structure with BHP doping. The plots of $(\alpha h\nu)^{1/2}$ versus hν are presented and compared in Fig. 4(a). Applying the technique presented in Eq. (3) can provide E_g values that are suitable for gas sensors and piezoelectric devices, among many other technical and scientific advantages [49].

As can be seen from Fig. 4(b), At the initial doping (0.1-0.8 mM), the BHP molecules themselves introduce new energy levels within the PVA bandgap, acting as localized states that are defects or impurities in the PVA matrix [50]. A considerable change in the energy band gap, from 5.32 eV for pure PVA to 3.38 eV for doped PVA, suggests that BHP molecules can alter the electronic structure of the PVA matrix by shifting energy states between the valence and conduction bands. The presence of localized states or defect levels in BHP can effectively reduce the energy gap, allowing for absorption of lower-energy photons. Furthermore, the strong hydrogen bonds between hydroxyls groups of BHPS and -OH chains of PVA change the density of states (DOS) around the band boundaries [51]. When there is 100% BHP concentration, the localized states can begin to overlap and saturate, leading to a decrease in the density of available states for electronic transitions. In addition, at very high concentrations, the BHP molecules may start to aggregate, thus leading to their excited states interacting and losing energy non-radiatively (without emitting light). The BHP clusters at higher concentrations (S_3, S_4) form structures close to quantum wells, which make excitonic transitions easier. The effect of the

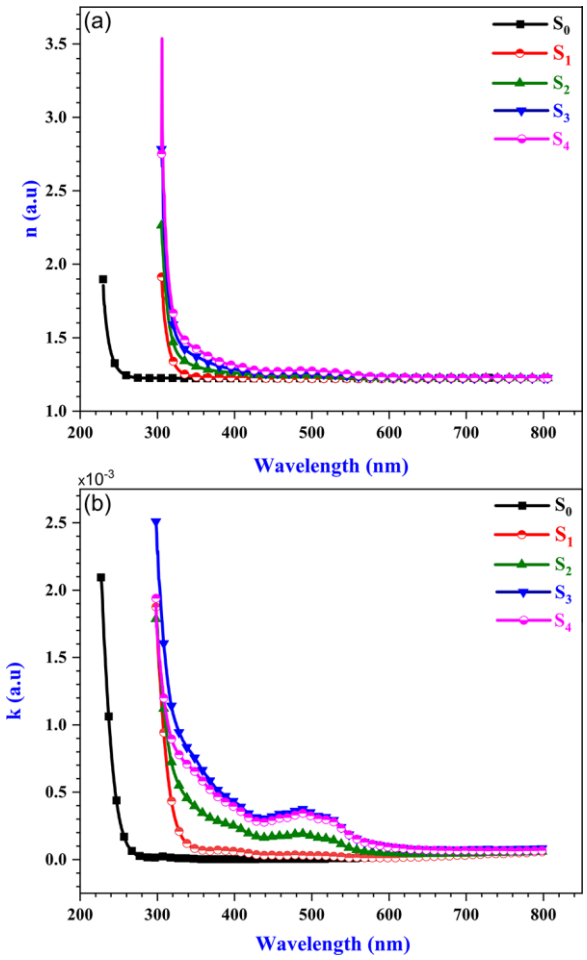

Fig.5. (a) Refractive index and (b) extinction coefficient versus wavelength of PVA and doped samples at various concentrations of BHP.

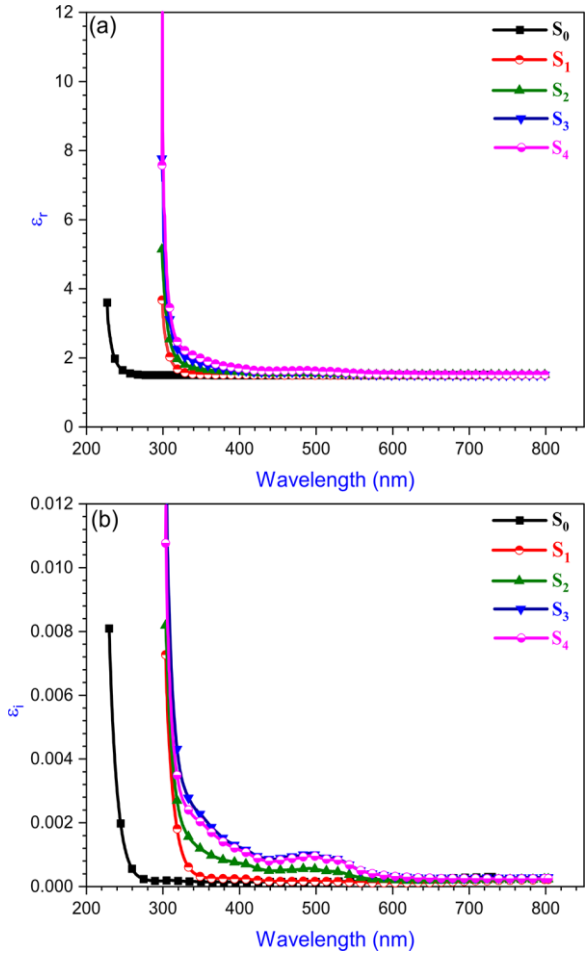

Fig.6. (a) Real and (b) imaginary parts of the dielectric function of PVA and doped samples at various concentrations of BHP.

new BHP molecules creates new localized energy levels within the band gap of the material, specifically below the conduction band. Localized states arising from structural or compositional defects lead to tail states that extend into the forbidden energy gap. These tail states can trap charge carriers, such as electrons or holes, depending on their nature. This behavior shows up in the absorption spectrum as an exponential The latter is commonly used as a measure of material disorder. As shown in Fig. 6, increasing the concentration of BHP induces electrostatic disorder within the PVA polymer chains. This increased disorder demonstrates a broadening of the Urbach tail and a higher E_u value. The enhancement of E_u makes sub-band gap absorption better for systems such as organic photovoltaics; however, charge carriers V move more slowly. F absorption edge known as the Urbach tail (E_u) move more slowly. F absorption edge known as the Urbach tail (E_u).

C. Refractive Index and Extinction Coefficient

As shown in Fig. 5(a), the refractive index generally decreases across the wavelength range for all dopant concentrations. Most transparent materials commonly exhibit this characteristic of normal dispersion. As can be seen in Fig. 5(a), the higher refractive index is observed at higher concentrations. Such a situation can result in increased light absorption and a higher refractive index due to the denser packing of molecules and enhanced polarizability. Furthermore, at higher concentrations, the

Table 2: A comparative analysis of the current work in relation to previously published studies.

Ref.	Fabrication Method	Bandgap Narrowing (ΔE_g)	Main Differences & Reasons
[50]	Solution casting of PVA/PVP blend doped with TPAI or THAI salt	~0.40 (with TPAI) and ~0.36 eV (with THAI)	Ionic doping instead of organic chromophore makes the bandgap larger and the electronic delocalization weaker.
[51]	Solution casting: PVA:SA blend doped with TiO_2	~0.30 eV	The TiO_2 surface has made the bandgap smaller, but it's still larger than BHP: PVA because inorganic particles add fewer mid-gap states.
[52]	Solution casting of PVA doped with Erythrosine EB dye	~0.50 eV	Doping with organic dye makes the bandgap smaller; however, not as substantially as BHP: PVA, it further decreases planarity and conjugation.
[53]	Solution blending and in-situ polymerization of PVA/PVP/PEDOT: PSS with NiO nanoparticles	~0.41 eV	Some reduction from conducting polymer and NiO, however higher than BHP: PVA; less efficient overlap of molecular orbitals.
[54]	Solution casting of PVA/NiO & PVA/CuO nanocomposites	~1.9 eV	Better than pure PVA, but greater than BHP: PVA; inorganic fillers generate less localized states.
Current work	Solution casting of PVA films doped with BHP	~2.0–2.22 eV	BHP has significant π-conjugation and substantial intermolecular interactions, which reduce the bandgap and enhance optical absorption.

probability of photon interaction with the dopant molecules increases. This higher interaction probability leads to a higher refractive index due to enhanced scattering and absorption phenomena.

The extinction coefficient (k) shown in Fig. 5(b) decreases with increasing wavelength. Higher concentrations of the dopant lead to a reduction of the extinction coefficient, particularly in the ultraviolet region. The addition of the dopant can affect the optical path length within the film. Moreover, higher concentrations may lead to a longer effective path length for light, which increases the likelihood of light absorption and changes the extinction coefficient.

D. Dielectric Response

Figure 6 represents the dielectric constant of PVA-doped film as a function of wavelength. The behavior of the real part of the dielectric constant (ε_r) can be explained by the interplay of dispersion, polarization, and electronic transitions (see Fig. 6(a)). Doping with BHP increases the dielectric constant by increasing the number of polar groups in the PVA matrix, which in turn leads to enhanced polarization. The dispersion region (~300-400 nm) reflects the electronic transitions within the material, where electrons can be excited from the valence band to higher energy levels. The absorption of photons in this region leads to a decrease in the dielectric constant. At longer wavelengths, the dielectric constant reaches a saturation region, indicating the maximum polarizability of the material. As shown in Fig. 6(b), increasing the concentration of the BHP dopant generally increases the imaginary part ε_i, particularly in the high-energy region. The resonance peaks at 3.4 eV for (S_3-S_4), attributed to the transitions $\pi \rightarrow \pi^*$ of BHP. This behavior implies that the dopant introduces additional energy levels into the PVA matrix, thereby facilitating photon passage by enhancing electron mobility between states. At longer wavelengths, photons can interact with certain electronic transitions linked to the BHP dopant. Such interaction causes absorption features typical of the dopant-PVA interaction.

E. Previous Studies and Real-World Applications

The behavior of the results from the current study is reasonable and aligns with some previous work [50-54]. To contextualize the

effects of BHP doping, we compare the result of the current study with published literature on PVA films doped with various chromophoric organic compounds, as detailed in Table 2.

The decreased bandgap calculation (–2.22 eV) exceeds the conventional values for doped PVA (–0.3 to –1.9 eV) [50-54]. This discrepancy can be attributed to the extended π-transition of BHP, which creates additional localized states near the conduction band. Additionally, BHP exhibits strong donor-acceptor behavior, along with enhanced molecular conjugation and electronic delocalization. The results in this work suggest that BHP: PVA is a favorable choice for optoelectronic applications since it has better bandgap engineering than doping with inorganic nanoparticles [51], [53], and [54], simple salts [50], or even other organic dyes [52].

The preparation method adopted, specifically solution casting in our study, is crucial as it determines the microstructure, which in turn affects the optical and electrical properties. This method has several advantages, including adjustability, cost-effectiveness, and compatibility with materials such as polymers, since it can be performed at low temperatures. Additionally, controlled evaporation during the casting process can facilitate the alignment of molecules, which reduces the bandgap and enhances the performance of the device, similar to the effects observed in polymer-based flexible devices.

This study shows that BHP: PVA blended films have a lot of promise for use in real-world optoelectronic applications, particularly because their bandgap can be changed (5.32–3.66 eV). These features make it possible to use UV and visible light photodetectors, flexible OLED displays, optical filters, nonlinear optical devices, and flexible solar cells or UV protection layers. This finding is consistent with previous research that shows how useful tunable organic semiconductors are in flexible electronics [50-54]. The technical features of BHP: PVA films make them suitable for innovative applications in wearable, rollable, and foldable optoelectronics, where softness, lightness, and configurable optical properties are essential.

V. CONCLUSIONS

The casting method was used at room temperature to create BHP-doped PVA films with silky, transparent, and uniform features. The films were analyzed using atomic force microscopy (AFM), histogram evaluation, amplitude distribution, and microscopic surface scans. The BHP-doped PVA films are solid, with no visible fractures or holes. A spectral range was used to evaluate the optical parameters of the produced BHP-doped PVA film, thereby indicating the complicated dielectric constant to be obtained. According to the results of optical characteristics, the binding of BHP with PVA polymers is another contribution to constructing polymer blends with reduced optical band gap energy. BHP doping causes significant optical modifications in PVA films: bandgap narrowing (–1.4 eV), Urbach energy increasing (+228%), and enhanced dielectric responses with distinguished excitonic peaks. These behaviors arise from the conjugated structure of BHP boost gap states, lattice disorder, and molecular polarization. The unique chemistry of BHP, unannealed film morphology, and specific characterization techniques help explain differences in literature. The tunable bandgap and dielectric properties make BHP/PVA a candidate for UV-visible photonics; however, Urbach broadening requires optimization for charge-transport applications.

ACKNOWLEDGMENTS

This research received some assistance from the Polymer Research Center (PRC) at the University of Basrah, which provided the researchers with essential exams and laboratory equipment.

REFERENCES

[1] C. Fleischmann, M. Lievenbrück, and H. Ritter, "Polymers and dyes: developments and applications", *Polymers*, vol. 7, no. 4, pp. 717–746, Apr. 2015.

[2] P. Meredith, C. J. Bettinger, M. Irimia-Vladu, A. B. Mostert, and P. E. Schwenn, "Electronic and optoelectronic materials and devices inspired by nature", *Rep. Prog. Phys*., vol. 76, no. 3, p. 034501, Feb. 2013.

[3] M. Shahid and F. Mohammad, "Recent advancements in natural dye applications: a review", *J. Clean. Prod*., vol. 53, pp. 310–331, Aug. 2013.

[4] F K. A. Patterson, C. M. Grimm, and T. M. Corsi, "Adopting new technologies for supply chain management", *Transp. Res. Part E Logist. Transp. Rev.*, vol. 39, no. 2, pp. 95–121, Mar. 2003.

[5] F. H. Malk, M. T. Obeed, and T. Alaridhee, "Optical characteristics of natural pigment of Portulaca grandiflora", *Proc. AIP Conf.*, AIP Publishing. Iraq, vol. 2977, pp. 040012, no. 1, Dec. 2023.

[6] T. Alaridhee, M. T. Obeed, F. H. Malk, and B. A. Dhahi, "Optical characteristics of Portulaca grandiflora-doped cellulose using the spray pyrolysis technique", *Opto-Electron. Rev*., vol. 31, Jul. 2023.

[7] D. Gounden, N. Nombona, and W. E. Van Zyl, "Recent advances in phthalocyanines for chemical sensor, non-linear optics (NLO) and energy storage applications", *Coord. Chem. Rev*., vol. 420, p. 213359, Oct. 2020.

[8] S. Parola, B. Julián-López, L. D. Carlos, and C. Sanchez, "Optical properties of hybrid organic-inorganic materials and their applications", *Adv. Funct. Mater*., vol. 26, no. 36, pp. 6506–6544, Sep. 2016

[9] T. A. Alaridhee, F. H. Malk, and A. A. Hussein, "Effect of static magnetic field on Anchusa italica-doped pentacene," *Mater. Sci. Forum*, vol. 1065, pp. 13–21, Jun. 2022.

[10] F. A. Tuma, M. T. Obeed, A. A. Jari, H. A. Badran, and T. A. Alaridhee, "Effect of gamma ray on self-induced diffraction patterns of organic compound poly (methyl-methacrylate) films," *Results in Phys*., vol. 52, pp. 106858, Sep. 2023.

[11] M. T. Obeed, T. A. Alaridhee, R. M. Abdullah, H. A. Badran, R. C. Abul-Hail, H. A. Hasan, and K. I. Ajeel, "Studies of third order nonlinearity and thermal diffusivity of C3OC dye using thermal lens technique," *Results in Phys*., vol. 66, pp. 108001, Nov. 2024.

[12] E. H. Nguyen, W. T. Daly, N. N. T. Le, M. Farnoodian, D. G. Belair, M. P. Schwartz, and W. L. Murphy, "Versatile synthetic alternatives to Matrigel for vascular toxicity screening and stem cell expansion", *Nature Biomedical Engineering,* vol. 1, pp. 0096, Jul. 2017.

[13] C. Sanchez, P. Belleville, M. Popall, and L. Nicole, "Applications of advanced hybrid organic–inorganic nanomaterials: from laboratory to market", *Chemical Society Reviews*, vol. 40, pp. 696-753, Feb. 2011.

[14] S. H. Mir, L. A. Nagahara, T. Thundat, P. Mokarian-Tabari, H. Furukawa, and A. Khosla, "Organic-inorganic hybrid functional materials: An integrated platform for applied technologies", *Journal of The Electrochemical Society*, vol. 165, pp. B3137-B3156, Jun. 2018.

[15] T. C. Tang, B. An, Y. Huang, S. Vasikaran, Y. Wang, X. Jiang, and C. Zhong, "Materials design by synthetic biology", *Nature Reviews Materials*, vol. 6, pp. 332-350, Apr. 2021.

[16] M. Beija, C. A. Afonso, and J. M. Martinho, "Synthesis and applications of Rhodamine derivatives as fluorescent probes", *Chemical Society Reviews*, vol. 38, pp. 2410-2433, Aug. 2009.

[17] S. H. Park, N. Kwon, J. H. Lee, J. Yoon, and I. Shin, "Synthetic ratiometric fluorescent probes for detection of ions", *Chemical Society Reviews*, vol. 49, pp. 143-179, Jan. 2020.

[18] J. A. Cotruvo Jr., A. T. Aron, K. M. Ramos-Torres, and C. J. Chang, "Synthetic fluorescent probes for studying copper in biological systems", *Chemical Society Reviews*, vol. 44, pp. 4400-4414, Jul. 2015.

[19] A. J. Kuehne and M. C. Gather, "Organic lasers: recent developments on materials, device geometries, and fabrication techniques", *Chemical Reviews*, vol. 116, pp. 12823-12864, Nov. 2016.

[20] Y. Jiang, Y. Y. Liu, X. Liu, H. Lin, K. Gao, W. Y. Lai, and W. Huang, "Organic solid-state lasers: A materials view and future development", *Chemical Society Reviews*, vol. 49, pp. 5885-5944, Aug. 2020.

[21] H. Abrahamse and M. R. Hamblin, "New photosensitizers for photodynamic therapy", *Biochemical Journal*, vol. 473, pp. 347-364, Feb. 2016.

[22] [21] A. Kamkaew, S. H. Lim, H. B. Lee, L. V. Kiew, L. Y. Chung, and K. Burgess, "BODIPY dyes in photodynamic therapy", *Chemical Society Reviews*, vol. 42, pp. 77-88, Jan. 2013.

[23] I. S. Yadav and R. Misra, "Design, synthesis and functionalization of BODIPY dyes: applications in dye-sensitized solar cells (DSSCs) and photodynamic therapy (PDT)",

Journal of Materials Chemistry C, vol. 11, pp. 8688-8723, Jul. 2023.

[24] A. S. Klymchenko, "Solvatochromic and fluorogenic dyes as environment-sensitive probes: design and biological applications", *Accounts of Chemical Research*, vol. 50, pp. 366-375, Feb. 2017.

[25] J. Tropp, M. H. Ihde, E. R. Crater, N. C. Bell, R. Bhatta, I. C. Johnson, and J. D. Azoulay, "A sensor array for the nanomolar detection of azo dyes in water", *ACS Sensors*, vol. 5, pp. 1541-1547, Jun. 2020.

[26] S. V. Kaymaz, H. M. Nobar, H. Sarıgül, C. Soylukan, L. Akyüz, and M. Yüce, "Nanomaterial surface modification toolkit: Principles, components, recipes, and applications", *Advances in Colloid and Interface Science*, vol. 322, pp. 103035, Dec. 2023.

[27] M. Ilakiyalakshmi, K. Dhanasekaran, and A. A. Napoleon, "A Review on Recent Development of Phenothiazine-Based Chromogenic and Fluorogenic Sensors for the Detection of Cations, Anions, and Neutral Analytes", *Topics in Current Chemistry*, vol. 382, pp. 29, Sep. 2024.

[28] C. McDonagh, C. S. Burke, and B. D. MacCraith, "Optical chemical sensors", *Chem. Rev*., vol. 108, no. 2, pp. 400–422, Jan. 2008.

[29] Y. Liu, Y. Zhong, and C. Wang, "Recent advances in self-actuation and self-sensing materials: State of the art and future perspectives," *Talanta*, vol. 212, p. 120808, May. 2020.

[30] K. Choi, A. H. C. Ng, R. Fobel, and A. R. Wheeler, "Digital microfluidics", *Annu. Rev. Anal. Chem.*, vol. 5, pp. 413–440, Jul. 2012.

[31] M. Aslam, M. A. Kalyar, and Z. A. Raza, "Polyvinyl alcohol: A review of research status and use of polyvinyl alcohol-based nanocomposites" *Polym. Eng. Sci*., vol. 58, no. 12, pp. 2119–2132, Dec. 2018.

[32] E. A. Kamoun, E. R. Kenawy, and X. Chen, "A review on polymeric hydrogel membranes for wound dressing applications: PVA-based hydrogel dressings", *J. Adv. Res*., vol. 8, no. 3, pp. 217-233, May. 2017.

[33] Y. Zhong, Q. Lin, H. Yu, L. Shao, X. Cui, Q. Pang, Y. Zhu, and R. Hou, "Construction methods and biomedical applications of PVA-based hydrogels", *Front. Chem.*, vol. 12, p. 1376799, Feb. 2024.

[34] F. Mark, *Optical properties of solids*, 2nd ed., Oxford university press, Feb. 2010.

[35] R. L. Sutherland, *Handbook of Nonlinear Optics*, 2nd ed., Boca Raton, FL, USA: CRC Press, Apr. 2003

[36] C. A. Hunter and J. K. Sanders, "The nature of π-π interactions", *J. Am. Chem. Soc*., vol. 112, no. 14, pp. 5525-5534, Jul. 1990.

[37] F. Würthner, T. E. Kaiser, and C. R. Saha-Möller, "J-aggregates: from serendipitous discovery to supramolecular engineering of functional dye materials", *Angew. Chem. Int. Ed.,* vol. 50, no. 15, pp. 3376-3410, Apr. 2011.

[38] Tauc and A. Menth, "States in the gap", *J. Non-Cryst. Solids*, vol. 8–10, pp. 569–585, Jun. 1972.

[39] F. Urbach, "The long-wavelength edge of photographic sensitivity and of the electronic absorption of solids", *Physical review*, vol. 92, no. 5, pp. 1324, Dec. 1953.

[40] C. Wakai, A. Oleinikova, M. Ott, and H. Weingärtner, "How polar are ionic liquids? Determination of the static dielectric constant of an imidazolium-based ionic liquid by microwave dielectric spectroscopy", *J. Phys. Chem. B*, vol. 109, no. 36, pp. 17028-17030, Aug. 2005.

[41] J. Rheims, J. Köser, and T. Wriedt, "Refractive-index measurements in the near-IR using an Abbe refractometer", *Meas. Sci. Technol*., vol. 8, no. 6, pp. 601, Jun. 1997.

[42] J M. J. Schnepf, M. Mayer, C. Kuttner, M. Tebbe, D. Wolf, M. Dulle, T. Altantzis et al., "Nanorattles with tailored electric field enhancement", *Nanoscale*, vol. 9, no. 27, pp. 9376-9385, Jun. 2017.

[43] E. D. Palik, *Handbook of Optical Constants of Solids,* 1st ed., Academic Press, San Diego, Jul. 1985.

[44] M. Born and E. Wolf, *Principles of Optics: Electromagnetic Theory of Propagation, Interference and Diffraction of Light*, 7th ed., Cambridge University Press, Apr. 2013.

[45] T. A. Alaridhee, Malk, F. H., Hussein, A. A., & Abid, D. S. "Enhanced absorption edge of Anchusa-Italica-doped pentacene towards optoelectronic applications", *Mater. Sci. Forum*, vol. 1002, pp. 251-263, Jul. 2020.

[46] Y. Hong, J. W. Y. Lam, and B. Z. Tang, "Aggregation-induced emission", *Chem. Soc. Rev*., vol. 40, no. 11, pp. 5361–5388, Jul. 2011.

[47] L. Duan et al., "Comparative study of light- and thermal-induced degradation for both fullerene and non-fullerene-based organic solar cells", *Sustain. Energy Fuels*, vol. 3, no. 3, pp. 723–735, Jan. 2019.

[48] K. M. Reddy, S. V. Manorama, and A. R. Reddy, "Bandgap studies on anatase titanium dioxide nanoparticles", *Mater. Chem. Phys*., vol. 78, no. 1, pp. 239–245, Feb. 2003.

[49] E. Ugur et al., "Life on the Urbach edge", *J. Phys. Chem. Lett*., vol. 13, no. 33, pp. 7702–7711, Aug. 2022.

[50] A. M. El-Naggar, S. Z. Brnawi, A. M. Kamal, A. A. Albassam, Z. K. Heiba, and M. B. Mohamed, "Structural, optical, and electrical parameters of doped PVA/PVP blend with TPAI or THAI salt", *Polymers*, vol. 15, no. 12, p. 2661, Jun. 2023.

[51] R. Khalil, N. A. Kelany, M. A. Ibrahim, G. M. Al-Senani, and A. M. Mostafa, "Linear and nonlinear optical properties of PVA:SA blend reinforced by TiO2 nanoparticles prepared by flower extract of aloe vera for optoelectronic applications", *Coatings*, vol. 13, no. 4, p. 699, Mar. 2023.

[52] E. F. El-Zaidia, H. A. Ali, T. A. Hamdalla, A. A. Darwish, and T. A. Hanafy, "Optical linearity and bandgap analysis of Erythrosine B doped in polyvinyl alcohol films", *Opt. Mater*., vol. 100, p. 109661, Feb. 2020.

[53] E. Salim, A. Magdy, A. H. El-Farrash, and A. El-Shaer, "Optimizing optical, dielectric, and electrical properties of polyvinyl alcohol/polyvinyl pyrrolidone/ poly (3,4-ethylene dioxythiophene) polystyrene sulfonate/NiO-based polymeric nanocomposites for optoelectronic applications", *Sci. Rep*., vol. 15, no. 1, p. 821, Jan. 2025.

[54] Z. Malik, A. Khattak, A. A. Alahmadi, and S. U. Butt, "Development and investigation of high performance PVA/NiO and PVA/CuO nanocomposites with improved physical, dielectric and mechanical properties", *Materials*, vol. 15, no. 15, pp. 5154, Jul. 2022.